Research Square

Preprints are preliminary reports that have not undergone peer review.
They should not be considered conclusive, used to inform clinical practice,
or referenced by the media as validated information.

A rising water table mobilizes deep, iron-bound soil phosphorus

Daniel Petticord

petticordd@caryinstitute.org

Cary Institute of Ecosystem Studies https://orcid.org/0000-0002-1764-6321

Benjamin Uveges

Cornell University https://orcid.org/0000-0002-8981-8970

Elizabeth Boughton

Archbold Biological Station

Rohit Fenn

Archbold Biological Station

Lucille Hentzen

Archbold Biological Station

Amartya Saha

Archbold Biological Station

Allasandra Valdez

Cornell University

Steven Wagner

Archbold Biological Station

Anna Wazny

Archbold Biological Station

Jed Sparks

Cornell University https://orcid.org/0000-0002-4333-1251

Article

Keywords:

Posted Date: October 1st, 2026

DOI: https://doi.org/10.21203/rs.3.rs-10896921/v1

License: This work is licensed under a Creative Commons Attribution 4.0 International License.
Read Full License

Additional Declarations: There is **NO** Competing Interest. We have no competing interests.

A rising water table mobilizes deep, iron-bound soil phosphorus

Daniel F. Petticord[1], Benjamin T. Uveges[1], Elizabeth H. Boughton[2], Rohit Fenn[2], Lucille M. Hentzen[2], Amartya Saha[2], Allasandra Valdez[1], Steven J. Wagner[2], Anna E. Wazny[2], Jed P. Sparks[1]

[1]Department of Ecology and Evolutionary Biology, Cornell University, Ithaca, NY, USA

[2]Archbold Biological Station, Venus, FL

Corresponding author: Daniel F. Petticord (petticordd@caryinstitute.org);

Abstract

Soil physiochemistry controls phosphorus (P) biogeochemistry and, by extension, plant productivity in terrestrial environments. Often, P is split into plant-available and bound pools. Iron-bound P, specifically, is traditionally considered unavailable to plants. Here we show iron-rich soil layers can hold the majority (60 to 78 percent) of phosphorus in the top meter of soil and, more importantly, when the rise of a seasonal water table reaches this layer the reductive dissolution of iron oxides releases high concentrations of P into soil pore water. Further, combining deep soil coring, ground-penetrating radar, and pore-water and groundwater monitoring across three subtropical pastures we found such fluxes are widespread, with 80-90% of the landscape overlying these deep P-retaining and redox sensitive layers. Importantly, the same dynamics we observe may arise wherever iron-rich subsoils are regularly exposed to shifting redox conditions — across many landscapes we currently consider to be phosphorus-poor. Future work must consider a) deep soils, b) seasonal fluctuations in nutrient availability, and c) the role of amorphous iron surfaces in upland soils as both sinks *and* as potential P sources during periods of shifting redox.

Introduction

As soils develop, phosphorus is progressively lost from the profile, and the P that remains is redistributed out of weatherable primary minerals (chiefly apatite) into organic forms and into association with secondary iron and aluminum (hydr)oxides, where a growing fraction becomes occluded and effectively inaccessible on ecological timescales (Walker and Syers 1976). Typically, the bioavailability of soil phosphorus is estimated by how easily P can be released into solution by a reagent. Iron-bound and occluded forms represent phosphorus generally considered less accessible to plants (Hedley et al. 1982; Cross and Schlesinger 1995).

A century of work, however, demonstrates that shifting redox conditions may dissolve ferric Fe, and in the process release P (Mortimer 1941; Patrick and Khalid 1974; Ponnamperuma 1972; Ruttenberg 2003). Much of this work stems from aquatic ecosystems, like wetlands and mangrove forests (Richardson 1985; Reddy and DeLaune 2008). However, we increasingly observe that plants may manipulate redox condition to 'mine' P from Fe minerals. For example, roots may create daily redox cycles that free Fe-bound P for uptake (Li et al. 2025). In low-P environments, grassland plants associated with iron-solubilizing fungi have higher %P content (Petticord et al 2026a). The role of microbes may be particularly important, as the decomposition of organic substrates can directly shift redox conditions or otherwise facilitate the reductive dissolution of Fe, freeing P into solution (Roden and Edmonds 1997; Lovley 1991).

Iron–phosphorus bonds are common, but are typically more important in acidic, weathered soils deplete of calcium phosphates, usually where precipitation outpaces evapotranspiration (Slessarev et al. 2016). Therefore, across wet, weathered ecosystems, a relatively large share of soil phosphorus may associate with redox-sensitive Fe surfaces. While these surfaces are widespread, the release of P from Fe can be difficult to observe in the field, because reactive Fe

46 is spread throughout the soil profile. Phosphorus freed at an anoxic site re-precipitates onto a
47 nearby undissolved Fe surface.

48 This diffuse re-trapping, sometimes called the 'iron trap' (Chambers and Odum 1990), can
49 immediately re-immobilize P at or near the original point of release. This re-immobilization
50 makes it difficult to track the release of P from redox-sensitive surfaces and would suggest the
51 ecological dynamics of such fluxes in upland soils are relatively unimportant. While the release
52 and re-precipitation of P provides a window for immediate immobilization into microbes, the
53 'iron trap' may diminish the likelihood such fluxes are reasonable provisions of P to the rooting
54 profile or to nearby waterbodies. This is especially true in deeper soils or sediments, where
55 redox-sensitive Fe-P bonds may be overtopped by additional soil layers rich in Fe.

56 However, at least one soil system exists where Fe surfaces are spatially isolated: the podzol. In a
57 podzol, intense weathering strips iron, aluminum, and phosphorus from the surface and re-
58 precipitates all three at depth in a single amorphous, redox-sensitive band, the spodic horizon
59 (Sauer et al. 2007). Importantly, because weathering has stripped the soil above the spodic of
60 cations, P released from Fe into a rising water table can rise into a cation-poor soil layer, where
61 there is no iron trap, and thus rise out of the spodic into the rooting zone (or possibly be
62 transported laterally through the cation-poor *E* layer).

63 Field and laboratory studies in podzols and analogous iron-rich soils have observed P release
64 with a rising water table, but none has closed the budget, resolved the mechanism, or measured
65 the extent at which such dynamics apply (Nair et al. 1999; Obour et al. 2011; Smith et al. 2021).
66 Presumably, reduction of the Fe surfaces during periods of flooding could explain the
67 intermittent flushes of dissolved P observed in soil pore water, but this has yet to be sufficiently
68 tested. In order to test these ideas and quantify the potential scale of P remobilization involved,

69 we used the podzols of the southeastern USA, where the spodic horizon lies within reach of a
70 strongly seasonal water table, as an exemplar system.

71 We worked across three pastures that represent two categories of landscape: historically
72 fertilized ground and a less intensively managed, semi-native site with no history of fertilization.
73 At each pasture we combined three measurements: 1)sampled pore water and groundwater
74 roughly monthly for eighteen months; 2) cored to one-meter to close a ‘deep’ P budget; and 3)
75 used ground-penetrating radar to trace the spodic horizon across the landscape, extrapolating our
76 point measurements to the pasture scale.

77 From this design we test three hypotheses. First, the buried spodic zone, not the topsoil, holds
78 most of the profile's P, and the signature of past fertilization shows more clearly in the deep
79 spodic than in the depleted surface soil. Second, a rising water table releases P from the spodic
80 by reducing iron, so dissolved P and dissolved Fe rise together above the horizon but stay flat
81 below the horizon. Third, the spodic is laterally continuous, so radar can map the horizon and
82 thus we may estimate where the water table overtops the spodic.

Results

A buried, iron-rich soil layer (the spodic) holds most of the P within the top meter of soil

Our geochemical analyses showed that most of the P in each profile was in the buried spodic zone (Fig. 1). The spodic is the upper of two P-fixing horizons: the humus-rich Bh, which overtops a sesquioxide-rich Bw. Together the Bh and Bw held a median of 78% of profile P at Managed Pasture 1, 74% at Managed Pasture 2, and 60% at Semi-Native Grassland (Fig. 1b). Within the shallower A-plus-Bh pool alone, the Bh held 73%, 74%, and 83% (Extended Data Table 3). The Bw was not a minor addition to the Bh. At Managed Pasture 1 the Bw held 424 kg P ha^{-1}, against 205 kg P ha^{-1} in the Bh. As areal stocks the spodic reserves were large: 629 kg P ha^{-1} at Managed Pasture 1, 104 at Semi-Native Grassland, and 168 at Managed Pasture 2, each several times the P of the overlying A horizon (Fig. 1b).

Consistent with expectations, the relic of previous fertilizer applications was more obvious at depth than in the surface soil. The two fertilized pastures (Managed Pasture 1 and Managed Pasture 2) held more P in the Bh than the semi-native pasture (Semi-Native Grassland) (median 62 versus 33 mg kg^{-1}; Wilcoxon $p = 0.015$), while the surface soils were uniformly P-poor. Other locations in this landscape, particularly Histosols and Alfisols where podzolization has not taken place, have higher surface P concentrations. This is likely because Fe and Al have not translocated to deeper in the soil profile, as is necessary for the formation of the spodic horizon on which we focus (Extended Data Fig. 1).

A rising water table releases P above the spodic

When the seasonal water table rose into the spodic, P concentrations in the pore water above the spodic rose, but there was no change in concentration beneath the spodic (Fig. 2). Soil pore water TP concentrations directly followed the water table through every wet-dry cycle, but only above the Bh (Fig. 2a; the underlying raw concentrations and water-table records are shown per site in Extended Data Fig. 2). Above the spodic horizon, a rising water table drove rising soil porewater TP concentrations by 3.7-fold at Managed Pasture 2, 2.6-fold at Semi-Native Grassland, and 1.9-fold at Managed Pasture 1, while staying flat or even decreasing below the spodic (water-table-by-position interaction $p = 0.0001$; three-way interaction with site $p = 0.0041$; Fig. 2b; per-site series in Extended Data Fig. 3).

We intentionally included a contrast meant to test if the remobilization we observe is an artifact of comparing the rooting zone against deep soils, or truly just an effect of position relative to the spodic horizon. At Managed Pasture 2, the deepest-spodic site, all lysimeters were installed above the spodic (one set near the rooting zone, and the paired lysimeters at approximately 70cm depth, just at the threshold of the spodic), so P releasing off the spodic should raise P concentrations at both, whereas a rooting-zone pulse should raise P only at the shallower position. Regardless of installation depth, above-spodic P rose with the water table as predicted (Fig. 2b).

We sampled for dissolved Fe in soil porewater as evidence for our proposed mechanism; namely that flooding shifts redox conditions, dissolving Fe surfaces and liberating P. At all above-spodic lysimeters, at all sites, the amount of released P was well predicted by the amount of dissolved iron. Above the Bh, dissolved total P rose and fell with dissolved Fe at every site (total-P–Fe Spearman $\rho = +0.27$ at Managed Pasture 2, +0.59 at Managed Pasture 1, +0.31 at Semi-Native Grassland; all $p < 0.05$), but showed no relation below the Bh (Fig. 2c; the orthophosphate companion is Extended Data Fig. 4). We present this as evidence P is released by the reductive dissolution of Fe oxides.

The spodic is laterally continuous across the landscape

We used ground penetrating radar to determine if the spodic horizons near the lysimeter installations represent real, landscape-scale features in deep soil, and to estimate variation in both depth and connectivity at the pasture scale. Our 750 MHz radar returned a coherent reflector at the top of the spodic (Fig. 3). Bridged coverage of the reflector was greater than 80% at all three sites: 92.8% at Managed Pasture 1, 85.0% at Managed Pasture 2, and 80.7% at Semi-Native Grassland. In some scans, we observed as the spodic gradually tracked upward, merging with the surface profile at the field margins, most plausibly where pastures intersect with neighboring Alfisols or Histosols, soil types that lack a spodic layer and where Fe and Al are retained at the surface (Extended Data Fig. 1). By matching our cores to the GPR transects, we found the GPR method had a mean absolute error of 13 cm and an R^2 of 0.61 (Fig. 3, inset).

The spodic ranged from 47 to 68 cm deep, meaning that in every case, the major subsidy of P for a one-meter profile would sit beneath a classic 10-30 cm coring effort (Figure 4).). Two other transects, one for Managed Pasture 2, one for Semi-Native Grassland, appear in Extended Data Fig. 5.

The buried reserve is large next to what a crop removes

The standing spodic reserve of plant-available M3-P, 104 to 629 kg P ha^{-1}, often exceeds the P of the surface A horizon several times over (Fig. 1b). Assuming the harvested export of a known forage crop is about 20 kg P ha^{-1} yr^{-1}, the spodic holds several years to several decades of removal with no resupply, 5 to 32 years across the sites (Extended Data Fig. 6a). Because the Bw continued below the base of the one-meter cores, these figures are conservative lower bounds.

Discussion

Across all sample locations, the buried spodic zone holds most of the profile's P. A rising water table drives the reductive dissolution of iron in that layer, which releases P, where it may be transported up through a non-reactive E horizon and into the rooting zone. To our knowledge, this is the first study to demonstrate that the oft-observed release of P during seasonal periods of flooding in this podzolized landscape may be the consequence of at least one particular mechanism – the reductive dissolution of Fe surfaces. In pore water, dissolved P rises and falls with dissolved Fe above the spodic (Fig. 2c). Within each site, the spodic layers richest in Fe underlay the lysimeters that release the most P (within-field Spearman $\rho = +0.83$; Extended Data Fig. 7b). As a caveat to these results, across our spodic samples aluminum outweighs Fe about forty-fold on a molar basis, and aluminum surfaces probably represent the larger share of sorbed P (Villapando and Graetz 2001; Extended Data Fig. 7a). The high concentration of aluminum in the spodic absolutely contributes to the high P loads of the spodic horizon. Aluminum, however, is not redox-sensitive. While it is possible hydrolysis or other mechanisms may liberate P from Al surfaces, we limit this study to focusing on evidence for the dissolution of Fe. Such dynamics are consistent with decades of evidence supporting Fe-P dynamics at the aquatic terrestrial interface, and a recent growing interest in the biotic manipulation of Fe in terrestrial ecosystems.

The presence of a deep P subsidy and accompanying seasonal release into flooded soils reconciles many observations from previous work in these landscapes, and may explain the consistently high concentrations of P in runoff, despite low surface P concentrations (Petticord et al. 2024, 2025; Qiu et al. 2024; Zhi et al. 2024). In a companion experiment in the same landscape, phytoremediation crops exported up to 20 kg P ha^{-1} yr^{-1}, substantially more than the surface soil and its inputs could supply (Petticord et al. 2026b).

The deep spodic is the only pool large enough to meet the previously observed demand, and the only pool both reactive and within reach of deep roots. Our approach does not yet allow for partitioning between advective transport of the P-enriched pore water versus direct mining of the solid-phase P of the spodic (Barber 1995). However, we note that our previous phytoremediation work found that the ideal remediation crop in this landscape (the crop which removed the most P in the form of biomass) is a thin-rooted *Hemarthria* sp. known to be wetland tolerant and well-adapted to flooded soils. The strong performance of a wetland-tolerant species adapted to maintain root activity in flooded soils is consistent with the emerging narrative that these redox-mobilized flushes of P represent an important component of annual growth and productivity. These findings have implications for management and conservation, our results suggest that targeted phytoremediation could help draw down legacy P in these landscapes reducing eutrophication risk [**Box 1**]. Left alone, the spodic reservoir would take centuries to millennia to eventually deplete – particularly where the deep reservoir has been 'loaded' by historic fertilization or land-use. However, our results suggest a deep-rooted, flood-adapted crop timed to the seasonal pulse can draw the reservoir down one to two orders of magnitude faster, and bring a pool that would otherwise persist for centuries within reach of a few decades of harvest (Extended Data Fig. 6b).

192 Legacy-P drawdown, and the protection of downstream waters, may therefore be better served
193 by phytoremediation aimed at the subsurface pulse alongside the surface practices now in place
194 (Newman and Pietro 2001).

Box 1: The role of the spodic horizon in managing water quality

The concentrations we measured have important consequences for surface water quality. During water table rise, total phosphorus in the rooting-zone pore water reached tens to hundreds of micrograms per liter, well above the levels at which surface waters eutrophy, and far above the 10 to 15 $\mu g\ L^{-1}$ target of the oligotrophic Everglades marsh downstream (Noe et al. 2001; Richardson et al. 2007). A redox-gated subsurface pathway that mobilizes legacy phosphorus from depth is therefore a plausible, and at present unmeasured, contributor to downstream loading. This pathway is distinct from the surface runoff that management has targeted. The very high concentrations observed in the Semi-Native Grassland raise a further possibility. Fertilized ground in this landscape, as across much of Florida, sits slightly above the surrounding lowlands. Phosphorus mobilized at depth beneath fertilized ground could move downslope through the subsurface toward lower sites such as Semi-Native Grassland. In reality, P need not stem directly from relic fertilizer – the semi-native landscapes could serve as subsurface 'catchments' for any surrounding 'highlands'. The idea that TP could be lifted up from the spodic, remobilized in subsurface flow, move unhindered through a cation-deplete *E* horizon, and be deposited 'downstream' is possible, but difficult to demonstrate. However, our observations show the highest concentrations of TP in porewater in our lowland site, which has never been fertilized. The movement of dissolved P away from historically managed lands and outward to neighboring landscapes is an environmental concern and should be further investigated. This downgradient path hypothesis would require a test including elevation and subsurface-flow, ideally coupled with tracer work. This is difficult, in part because P lacks a stable isotope that can be reliably used for tracing efforts, but future work chasing either the oxygen isotope of phosphate (Tamburini et al. 2014) or directly tracking the origin of P via uranium isotopes (Zielinski et al. 2000) provides valuable opportunities for such a study.

195 Subsurface transport of P is directly relevant to dispersed water management in south Florida,
196 where shallow rehydration of ranchlands and former agricultural uplands is intended to retain
197 water on-farm, slow overland flow, and reduce downstream nutrient loading (Bohlen and
198 Villapando 2011). Modeling studies suggest that water retention can reduce P export by up to
199 19% (Zhang et al. 2006), and keeping water on the landscape may extend the window for plant
200 uptake of mobilized P. However, our results suggest that inundation of spodic soils could
201 increase the release of P that may be vulnerable to loss via subsurface pathways. Future work
202 should consider directly monitoring groundwater or shallow subsurface flow (Aldous et al. 2005;
203 Zak et al. 2010).

204 There are perhaps two limitations within this work. First, we measured pore-water concentrations
205 and a mass-balance deficit, not a direct in-situ flux given the difficulty of tracking P to reliably
206 report flux. Our contribution is mainly to locate the source and the mechanism. Second, we urge
207 caution about the broader applicability of our proposed mechanism – this is only one site. Other
208 podzols that are more crystalline and are less redox-sensitive, or in which Fe surfaces are less
209 accessible to be loaded by P, may not reflect the same dynamic.

210 However, if one does scale our observations to a global relevance, we note that globally most
211 soil sampling miss the depth at which the spodic sits (Fig. 4). The most recent global total-P
212 synthesis suggests soils hold more than twice the P in the subsoil as in the topsoil worldwide
213 (62.2 versus 26.8 Pg below and above 30 cm), yet only about 14% of soil observations extend
214 below 30 cm (He et al. 2021). For Spodosols in particular (5% of the Earth's surface), the global
215 record reaches the 30-to-70 cm interval in fewer than one sample in five, at a median sampling
216 depth near 10 cm (He et al. 2023, extending Hou et al. 2018; Fig. 4, inset).

217

If redox-sensitive deep iron-bound P is real and quantitatively important, a number of systems we have called P-poor deserve greater scrutiny. Acidic, weathered soils where an iron-rich horizon sits within reach of a fluctuating water table, such as the tropical podzols of the Amazon, the seasonally flooded savannas of the Cerrado and West Africa, and the iron-rich coastal soils of the wet tropics are the clearest cases (Fig. 4). We suggest soil P science deserves a renaissance of ideas, much like our shift in understanding the persistence of organic matter as a property of environment rather than of molecular form (Schmidt et al. 2011; Lehmann and Kleber 2015). The first step is to sample deeper, and more frequently. Shifting towards measuring the concentration of dissolved ions in porewater, rather than just static stocks in dry soils, will also greatly enhance our understanding of how P cycles in these landscapes.

Acknowledgement

This research is a contribution from the United States Department of Agriculture Agricultural Research Service (USDA-ARS) Long-Term Agroecosystem Research (LTAR) network. Any opinions, findings, conclusion, or recommendations expressed in this publication are those of the author(s) and do not necessarily reflect the view of the USDA. This research was supported in part by the Everglades foundation, via The Micky and Madeleine Arison Family Foundation Everglades fellowship. Any opinions, findings, conclusion, or recommendations expressed in this publication are those of the author(s) and do not necessarily reflect the view of the Everglades Foundation or the Arison family. This work was supported in part by the Cornell Atkinson Center for Sustainability.

Methods

Study sites and design. Research was conducted at Archbold Biological Station's Buck Island Ranch, a commercial cattle operation and a site within the U.S. Department of Agriculture's (USDA) Long- Term Agroecosystem Research (LTAR) network in south-central Florida. The climate is humid, typically subtropical, with a wet summer, a dry winter, and a water table that rises and falls by season. We selected three sites. Two are historically 'heavily-managed' pastures with a history of P fertilization, Managed Pasture 1 and Managed Pasture 2. The third, Semi-Native Grassland, is a less intensively managed, semi-native pasture that has never been fertilized. All three sites contain podzols. The spodic horizon lies between 47 and 68 cm across the sites, and the seasonal water table reaches into or above the spodic for part of each year. The design held two contrasts. The first contrast set the two fertilized pastures against the semi-native pasture, to test whether the buried spodic carries a legacy of fertilization that the depleted surface no longer records. The second contrast served as an in-field control and is described with the lysimeter network below.

Deep coring and soil chemistry. At each site we collected soil cores to one meter on a spatial grid (Managed Pasture 1 n = 12, Managed Pasture 2 n = 8, Semi-Native Grassland n = 5). We split each core by horizon (A, E, Bh, Bw) and analyzed each horizon for Mehlich-3 P, iron, and aluminum, for pH, as well as the derived soil P storage capacity (SPSC) (Mehlich 1984; Nair et al. 2004; Nair and Harris 2004). All soil analyses were ultimately conducted using local IFAS extension laboratories, whose methodology is extensively documented elsewhere (Qiu 2024, Petticord 2026).

Cores beside the lysimeters. To tie the solid-phase chemistry of the spodic to the P released nearby, we also collected cores beside each lysimeter cluster (3-4 cores per cluster) and analyzed

each horizon for Mehlich-3 P, iron, and aluminum, and for pH. We report Mehlich-3 extractable P (M3-P) rather than total P. M3-P is the basis of the soil P storage capacity (SPSC) used across Florida. The extractant for M3-P, which combines dilute acid, fluoride, and EDTA, is intended to liberate P from the iron- and aluminum-bound P that dominates acid soils and indeed the spodic, but may not be perfectly effective. M3-P is therefore not an inventory of total P, and does not necessarily recover the iron-associated pool completely. M3-P does, however, predict the P that moves into water. Soil-test P does predict dissolved P in runoff and leachate across a wide range of soils (Sharpley 1995; Maguire and Sims 2002; Vadas et al. 2005). At this landscape, M3-P and total P covary in surface soils (rho = 0.84; Qiu et al. 2024). Still, it is important to understand these calibrations come from surface soils, so extending M3-P to a Bh or Bw at 50 to 100 cm is in some senses an extrapolation

Thus, because M3-P may recover only part of the total P pool, and because the Bw was the deepest horizon in every core that reached the Bw, the reserves we report are conservative lower bounds on the extractable stock, particularly at Managed Pasture 2, where in places a 1m core barely reached the spodic. The Bw was captured within the one-meter cores more often at Managed Pasture 1 than at Managed Pasture 2 or Semi-Native Grassland, so the between-field differences in absolute reserve partly reflect coring recovery rather than reservoir size alone. If we make some assumptions for unrecovered Bw concentrations based on per-fields mean recovered Bw, we may estimate the spodic reserves hold at least 120, 206, and 770 kg P ha^{-1} at Semi-Native Grassland, Managed Pasture 2, and Managed Pasture 1.

Areal Plant-available P reserves. We computed a per-horizon P stock (areal reserve) as the thickness-weighted mean Mehlich-3 P, times an assumed horizon bulk density (1.3 g cm^{-3} for

the A horizon, 1.2 g cm^{-3} for the E, Bh, and Bw), times the horizon thickness. We averaged each reserve over the cores in which the horizon was present and set 95% confidence intervals by bootstrap resampling (2,000 resamples). The spodic reserve is the sum of the Bh and Bw reserves. The Bw was the deepest horizon in every core that reached the Bw, so the base of the Bw was not always sampled. The Bw reserve, and therefore the spodic reserve, is a lower bound. The lower bound is most severe at Managed Pasture 2, where the deepest Bh left the least spodic material within the one-meter core.

Pore-water and groundwater monitoring. At each site we installed 12 stainless-steel tension lysimeters [manufacturer and model?] in clusters, at two depths: six shallow lysimeters in the rooting zone (between 20-40 cm) and six deep lysimeters (between 60-80 cm). We placed each lysimeter relative to the top of the Bh, so that a lysimeter sat either above or below the spodic. We sampled the lysimeters on biweekly to monthly intervals for eighteen months and measured total P, and dissolved Fe in each sample. We substituted non-detects at half the reporting limit, 2 μg L^{-1}, from a 4 μg L^{-1} limit. Water samples were all analyzed through local IFAS offices, whose methodologies are documented elsewhere (IFAS, Petticord 2026). We recorded water-table elevation at on-site wells and gap-filled each record to a daily series. The three sites lie close together on effectively flat ground and share a common regional water table, so we treated them as a single hydrological unit.

One well recorded continuously across the whole sampling period, while the other two records contain gaps. We therefore used our most-complete well's daily series as the water-table predictor at all three sites, which keeps every observation on one consistent series. We do display the well data for each site individually in Extended Data figures 2-4. We defined water-table contact as the table standing at or above the top of the Bh.

At the fertilized site with the deepest spodic, both lysimeters of a pair sit above the Bh: one in the rooting zone and one just above the top of the spodic, near 70 to 80 cm. A true remobilization off the spodic should raise P at both lysimeters, because both draw water that has passed above the spodic. A rooting-zone process, such as a pulse of biological activity, should raise P only at the shallow, rooting-zone lysimeter. The two mechanisms make different predictions, so the paired above-spodic lysimeters separate the mechanisms.

Ground-penetrating radar. ran radar survey transects at each site with a

MALÅ GX750 Ground Explorer, equipped with a 750 MHz antenna, running at least eight transects per site and roughly eight kilometers of line per site, about twenty-four kilometers in total. The top of the spodic produces a strong dielectric contrast, meaning it may present a strong reflector in the GPR output (Davis and Annan 1989; Collins and Doolittle 1987; Zajícová and Chuman 2019). We tracked the reflector along each transect with a Viterbi dynamic-programming algorithm (Viterbi 1967; Berger et al. 2019), initialized from the mean Bh depth of that site's cores. We converted travel time to depth with a constant radar velocity of 0.060 m ns^{-1}. We validated the radar picks against sixteen cores that could match to the transects, and obtained a mean absolute error of 13 cm and an R^2 of 0.61.

Statistical analysis. We modeled pore-water total P, log-transformed, with a linear mixed-effects model. The fixed effects were water-table depth, lysimeter installation depth (shallow, near 40 cm; deep, near 80 cm), site, and their interactions.

At Managed Pasture 1 and Semi-Native Grassland, lysimeters are installed above and below the spodic horizon. At Managed Pasture 2 both depths sit above the Bh by design, as the in-field control, so that site contributes no below-Bh observations. Random effects were crossed intercepts for individual lysimeter and for sampling date (n = 347). We report Type-III tests of

the fixed effects and treat the pre-specified water-table-by-position interaction as the primary inference. Where distributions were skewed or censored, we used non-parametric tests (Mann-Whitney, Wilcoxon, and Spearman) and report the uncorrected p-values as corroborating rather than independent. We assessed the timing of the response by cross-correlating above-Bh P with water-table position at monthly resolution. For the iron-versus-aluminum question, we computed molar iron-to-aluminum ratios in the spodic samples, and, across clusters, related the Fe content of each near-lysimeter Bh core to the mean above-Bh pore-water P of the adjacent lysimeters (Spearman, within site). We ran all analyses in R 4.4.1, with lme4 for the mixed model (R Core Team 2024; Bates et al. 2015).

Global reanalysis and companion budget. To frame our results within a global context, we used the global Hedley P compilation of He et al. (2023), which extends the database of Hou et al. (2018), and analyzed the distribution of sampling depths. For the drawdown and years-of-supply comparisons (Extended Data Fig. 6b), we took the harvested P export of a flood-adapted forage crop, *Hemarthria altissima*, at about 20 kg P ha^{-1} yr^{-1}, from the companion P budget at the same landscape (Petticord et al. 2026b).

Data availability

The processed data supporting these findings — soil chemistry, paired pore-water and groundwater time series, profile geometry and P stocks, ground-penetrating-radar picks, and the derived reserve, correlation and mixed-model outputs — will be made available via Figshare. Externally sourced datasets are the global Hedley fractionation compilation of He et al. (2023, extending Hou et al. 2018), the global total-P synthesis of He et al. (2021), and the companion P budget of Petticord et al. (2026b).

Code availability

The full analysis pipeline — data cleaning, the linear mixed-effects model, the ground-penetrating-radar reflector tracker, the bootstrap reserve estimation, and all figure-generation scripts (R) — will be deposited via the Code Ocean platform [DOI, to be assigned].

Author Contribution Statement

D.F.P. conceived the study, designed the methods, wrote the analysis code, carried out the field and laboratory work, performed the formal analysis, curated the data, produced the figures, administered the project, and wrote the original draft. B.T.U. contributed to design the methods, conceptualization, the field investigation and edited the manuscript. E.H.B. and J.P.S. contributed concepts, provided resources and funding, supervised the work, and edited the manuscript. R.F., L.M.H., A.V., S.J.W., and A.E.W. contributed to the field investigation and to editing the manuscript. All authors reviewed and approved the manuscript.

References

Aldous, A., McCormick, P., Ferguson, C., Graham, S., Craft, C. (2005). Hydrologic regime controls soil phosphorus fluxes in restoration and undisturbed wetlands. Restoration Ecology 13(2), 341–347. https://doi.org/10.1111/j.1526-100X.2005.00043.x

Barber, S.A. (1995). Soil Nutrient Bioavailability: A Mechanistic Approach. 2nd edn. John Wiley & Sons, New York.

Bates, D., Mächler, M., Bolker, B., Walker, S. (2015). Fitting linear mixed-effects models using lme4. Journal of Statistical Software 67(1), 1–48. https://doi.org/10.18637/jss.v067.i01

Berger, V., Xu, M., Al-Ibadi, M., Chu, S., Crandall, D., Paden, J. et al. (2019). Automated ice-bottom tracking of 2D and 3D ice radar imagery using Viterbi and TRW-S. IEEE Journal of Selected Topics in Applied Earth Observations and Remote Sensing 12(9), 3272–3285. https://doi.org/10.1109/JSTARS.2019.2930920

Chambers, R.M., Odum, W.E. (1990). Porewater oxidation, dissolved phosphate and the iron curtain. Biogeochemistry 10(1), 37–52. https://doi.org/10.1007/BF00000891

Collins, M.E., Doolittle, J.A. (1987). Using ground-penetrating radar to study soil microvariability. Soil Science Society of America Journal 51(2), 491–493. https://doi.org/10.2136/sssaj1987.03615995005100020045x

Cross, A.F., Schlesinger, W.H. (1995). A literature review and evaluation of the Hedley fractionation: applications to the biogeochemical cycle of soil phosphorus in natural ecosystems. Geoderma 64(3–4), 197–214. https://doi.org/10.1016/0016-7061(94)00023-4

Davis, J.L., Annan, A.P. (1989). Ground-penetrating radar for high-resolution mapping of soil and rock stratigraphy. Geophysical Prospecting 37(5), 531–551. https://doi.org/10.1111/j.1365-2478.1989.tb02221.x

Hedley, M.J., Stewart, J.W.B., Chauhan, B.S. (1982). Changes in inorganic and organic soil phosphorus fractions induced by cultivation practices and by laboratory incubations. Soil Science Society of America Journal 46(5), 970–976. https://doi.org/10.2136/sssaj1982.03615995004600050017x

He, X., Augusto, L., Goll, D.S., Ringeval, B., Wang, Y.-P. et al. (2021). Global patterns and drivers of soil total phosphorus concentration. Earth System Science Data 13(12), 5831–5846. https://doi.org/10.5194/essd-13-5831-2021

He, X., Augusto, L., Goll, D.S., Ringeval, B., Wang, Y.-P. et al. (2023). Global patterns and drivers of phosphorus fractions in natural soils. Biogeosciences 20(19), 4147–4163. https://doi.org/10.5194/bg-20-4147-2023

Hou, E., Tan, X., Heenan, M., Wen, D. (2018). A global dataset of plant available and unavailable phosphorus in natural soils derived by Hedley method. Scientific Data 5, 180166. https://doi.org/10.1038/sdata.2018.166

Lehmann, J., Kleber, M. (2015). The contentious nature of soil organic matter. Nature 528(7580), 60–68. https://doi.org/10.1038/nature16069

Li, C., Sheng, H., Tan, M., Dai, H., Wang, X. et al. (2025). Rhythmic radial oxygen loss enhances soil phosphorus bioavailability. Nature Communications 16, 4413. https://doi.org/10.1038/s41467-025-59637-x

Lovley, D.R. (1991). Dissimilatory Fe(III) and Mn(IV) reduction. Microbiological Reviews 55(2), 259–287. https://doi.org/10.1128/mr.55.2.259-287.1991

McDowell, R.W., Noble, A., Pletnyakov, P., Haygarth, P.M. (2023). A global database of soil plant available phosphorus. Scientific Data 10, 125. https://doi.org/10.1038/s41597-023-02022-4

McDowell, R.W., Noble, A.D.L., Doscher, C., Helfenstein, J. (2026). An improved global database and model of plant available soil phosphorus. Scientific Data 13, 880. https://doi.org/10.1038/s41597-026-07140-3

Maguire, R.O., Sims, J.T. (2002). Measuring agronomic and environmental soil phosphorus saturation and predicting phosphorus leaching with Mehlich 3. Soil Science Society of America Journal 66(6), 2033–2039. https://doi.org/10.2136/sssaj2002.2033

Mehlich, A. (1984). Mehlich 3 soil test extractant: a modification of Mehlich 2 extractant. Communications in Soil Science and Plant Analysis 15(12), 1409–1416. https://doi.org/10.1080/00103628409367568

Montes, C.R., Lucas, Y., Pereira, O.J.R., Achard, R., Grimaldi, M., Melfi, A.J. (2011). Deep plant-derived carbon storage in Amazonian podzols. Biogeosciences 8(1), 113–120. https://doi.org/10.5194/bg-8-113-2011

Mortimer, C.H. (1941). The exchange of dissolved substances between mud and water in lakes. Journal of Ecology 29(2), 280–329. https://doi.org/10.2307/2256395

Nair, V.D., Villapando, R.R., Graetz, D.A. (1999). Phosphorus retention capacity of the spodic horizon under varying environmental conditions. Journal of Environmental Quality 28(4), 1308–1313. https://doi.org/10.2134/jeq1999.00472425002800040035x

Nair, V.D., Harris, W.G. (2004). A capacity factor as an alternative to soil test phosphorus in phosphorus risk assessment. New Zealand Journal of Agricultural Research 47(4), 491–497. https://doi.org/10.1080/00288233.2004.9513616

Nair, V.D., Portier, K.M., Graetz, D.A., Walker, M.L. (2004). An environmental threshold for degree of phosphorus saturation in sandy soils. Journal of Environmental Quality 33(1), 107–113. https://doi.org/10.2134/jeq2004.1070

Newman, S., Pietro, K. (2001). Phosphorus storage and release in response to flooding: implications for Everglades stormwater treatment areas. Ecological Engineering 18(1), 23–38. https://doi.org/10.1016/S0925-8574(01)00063-5

Noe, G.B., Childers, D.L., Jones, R.D. (2001). Phosphorus biogeochemistry and the impact of phosphorus enrichment: why is the Everglades so unique?. Ecosystems 4(7), 603–624. https://doi.org/10.1007/s10021-001-0032-1

Obour, A.K., Silveira, M.L., Vendramini, J.M.B., Sollenberger, L.E., O'Connor, G.A. (2011). Fluctuating water table effect on phosphorus release and availability from a Florida Spodosol. Nutrient Cycling in Agroecosystems 91(2), 207–217. https://doi.org/10.1007/s10705-011-9456-y

Patrick, W.H., Khalid, R.A. (1974). Phosphate release and sorption by soils and sediments: effect of aerobic and anaerobic conditions. Science 186(4158), 53–55. https://doi.org/10.1126/science.186.4158.53

Petticord, D.F., Boughton, E.H., Li, H., Qiu, J., Saha, A., Zhi, R. et al. (2024). Planted species influences soil phosphorus losses in a historically fertilized pasture system: a mesocosm study. Ecosphere 15(9), e4976. https://doi.org/10.1002/ecs2.4976 (optional continuity self-cite)

Petticord, D.F., Uveges, B.T., Boughton, E.H., Strahm, B.D., Sparks, J.P. (2025). Spatial decoupling of biological and geochemical phosphorus cycling in podzolized soils. Soil Systems 9(4), 115. https://doi.org/10.3390/soilsystems9040115

Petticord, D.F., Zhi, R., Boughton, E.H., Guo, Y., Liao, H.-L., Reyes, A.L. et al. (2026a). Foliar phosphorus concentrations in Bahiagrass are well-predicted by the abundance of a Fusarium taxa. Soil Biology and Biochemistry 214, 110049. https://doi.org/10.1016/j.soilbio.2025.110049

Petticord, D.F., Boughton, E.H., Gough, A., Qiu, J., Reyes, A.L., Saha, A. et al. (2026b). Phosphorus mitigation through hay harvest: addressing legacy P in subtropical pasture. Agriculture, Ecosystems & Environment 399, 110136. https://doi.org/10.1016/j.agee.2025.110136

Ponnamperuma, F.N. (1972). The chemistry of submerged soils. In Advances in Agronomy (pp. 29–96). https://doi.org/10.1016/S0065-2113(08)60633-1

Qiu, J., Zhi, R., Boughton, E.H., Li, H., Henderson, C.R.B., Petticord, D.F. et al. (2024). Unraveling spatial heterogeneity of soil legacy phosphorus in subtropical grasslands. Ecological Applications 34(6), e3007. https://doi.org/10.1002/eap.3007 (optional continuity self-cite)

R Core Team (2024). R: A Language and Environment for Statistical Computing. R Foundation for Statistical Computing, Vienna, Austria.

Reddy, K.R., DeLaune, R.D. (2008). Biogeochemistry of Wetlands: Science and Applications. CRC Press, Boca Raton, FL. https://doi.org/10.1201/9780203491454

Richardson, C.J. (1985). Mechanisms controlling phosphorus retention capacity in freshwater wetlands. Science 228(4706), 1424–1427. https://doi.org/10.1126/science.228.4706.1424

Richardson, C.J., King, R.S., Qian, S.S., Vaithiyanathan, P., Qualls, R.G., Stow, C.A. (2007). Estimating ecological thresholds for phosphorus in the Everglades. Environmental Science & Technology 41(23), 8084–8091. https://doi.org/10.1021/es062624w

Roden, E.E., Edmonds, J.W. (1997). Phosphate mobilization in iron-rich anaerobic sediments: microbial Fe(III) oxide reduction versus iron-sulfide formation. Archiv für Hydrobiologie 139(3), 347–378. https://doi.org/10.1127/archiv-hydrobiol/139/1997/347

Rothe, M., Kleeberg, A., Hupfer, M. (2016). The occurrence, identification and environmental relevance of vivianite in waterlogged soils and aquatic sediments. Earth-Science Reviews 158, 51–64. https://doi.org/10.1016/j.earscirev.2016.04.008

Ruttenberg, K.C. (2003). The global phosphorus cycle. In Treatise on Geochemistry (eds Holland, H.D. & Turekian, K.K.), Vol. 8 (pp. 585–643). Elsevier. https://doi.org/10.1016/B0-08-043751-6/08153-6

Sauer, D., Sponagel, H., Sommer, M., Giani, L., Jahn, R., Stahr, K. (2007). Podzol: soil of the year 2007. A review on its genesis, occurrence, and functions. Journal of Plant Nutrition and Soil Science 170(5), 581–597. https://doi.org/10.1002/jpln.200700135

Schmidt, M.W.I., Torn, M.S., Abiven, S., Dittmar, T., Guggenberger, G. et al. (2011). Persistence of soil organic matter as an ecosystem property. Nature 478(7367), 49–56. https://doi.org/10.1038/nature10386

Sharpley, A.N. (1995). Dependence of runoff phosphorus on extractable soil phosphorus. Journal of Environmental Quality 24(5), 920–926. https://doi.org/10.2134/jeq1995.00472425002400050020x

Slessarev, E.W., Lin, Y., Bingham, N.L., Johnson, J.E., Dai, Y., Schimel, J.P., Chadwick, O.A. (2016). Water balance creates a threshold in soil pH at the global scale. Nature 540(7634), 567–569. https://doi.org/10.1038/nature20139

Smith, G.J., McDowell, R.W., Condron, L.M., Daly, K., Ó hUallacháin, D., Fenton, O. (2021). Reductive dissolution of phosphorus associated with iron-oxides during saturation in agricultural soil profiles. Journal of Environmental Quality 50(5), 1207–1219. https://doi.org/10.1002/jeq2.20256

Tamburini, F., Pfahler, V., von Sperber, C., Frossard, E., Bernasconi, S.M. (2014). Oxygen isotopes for unraveling phosphorus transformations in the soil-plant system: a review. Soil Science Society of America Journal 78(1), 38–46. https://doi.org/10.2136/sssaj2013.05.0186dgs

Vadas, P.A., Kleinman, P.J.A., Sharpley, A.N., Turner, B.L. (2005). Relating soil phosphorus to dissolved phosphorus in runoff: a single extraction coefficient for water quality modeling. Journal of Environmental Quality 34(2), 572–580. https://doi.org/10.2134/jeq2005.0572

Villapando, R.R., Graetz, D.A. (2001). Phosphorus sorption and desorption properties of the spodic horizon from selected Florida Spodosols. Soil Science Society of America Journal 65(2), 331–339. https://doi.org/10.2136/sssaj2001.652331x

Viterbi, A.J. (1967). Error bounds for convolutional codes and an asymptotically optimum decoding algorithm. IEEE Transactions on Information Theory 13(2), 260–269. https://doi.org/10.1109/TIT.1967.1054010

Walker, T.W., Syers, J.K. (1976). The fate of phosphorus during pedogenesis. Geoderma 15, 1–19. https://doi.org/10.1016/0016-7061(76)90066-5

Zajícová, K., Chuman, T. (2019). Application of ground penetrating radar methods in soil studies: a review. Geoderma 343, 116–129. https://doi.org/10.1016/j.geoderma.2019.02.024

Zak, D., Wagner, C., Payer, B., Augustin, J., Gelbrecht, J. (2010). Phosphorus mobilization in rewetted fens: the effect of altered peat properties and implications for their restoration. Ecological Applications 20(5), 1336–1349. https://doi.org/10.1890/08-2053.1

Zhi, R., Boughton, E.H., Li, H., Petticord, D.F., Saha, A., Sparks, J.P. et al. (2024). Soil legacy phosphorus and loss risk in subtropical grasslands. Journal of Environmental Management 366, 121656. https://doi.org/10.1016/j.jenvman.2024.121656 (optional continuity self-cite)

Zielinski, R.A., Simmons, K.R., Orem, W.H. (2000). Use of 234U and 238U isotopes to identify fertilizer-derived uranium in the Florida Everglades. Applied Geochemistry 15(3), 369–383. https://doi.org/10.1016/S0883-2927(99)00053-0

Figure legends

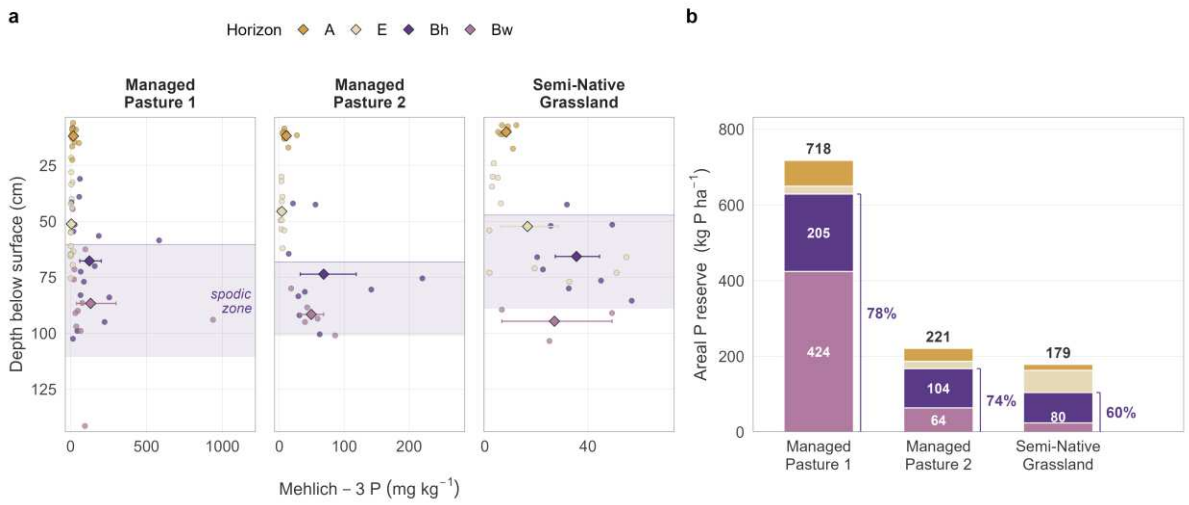
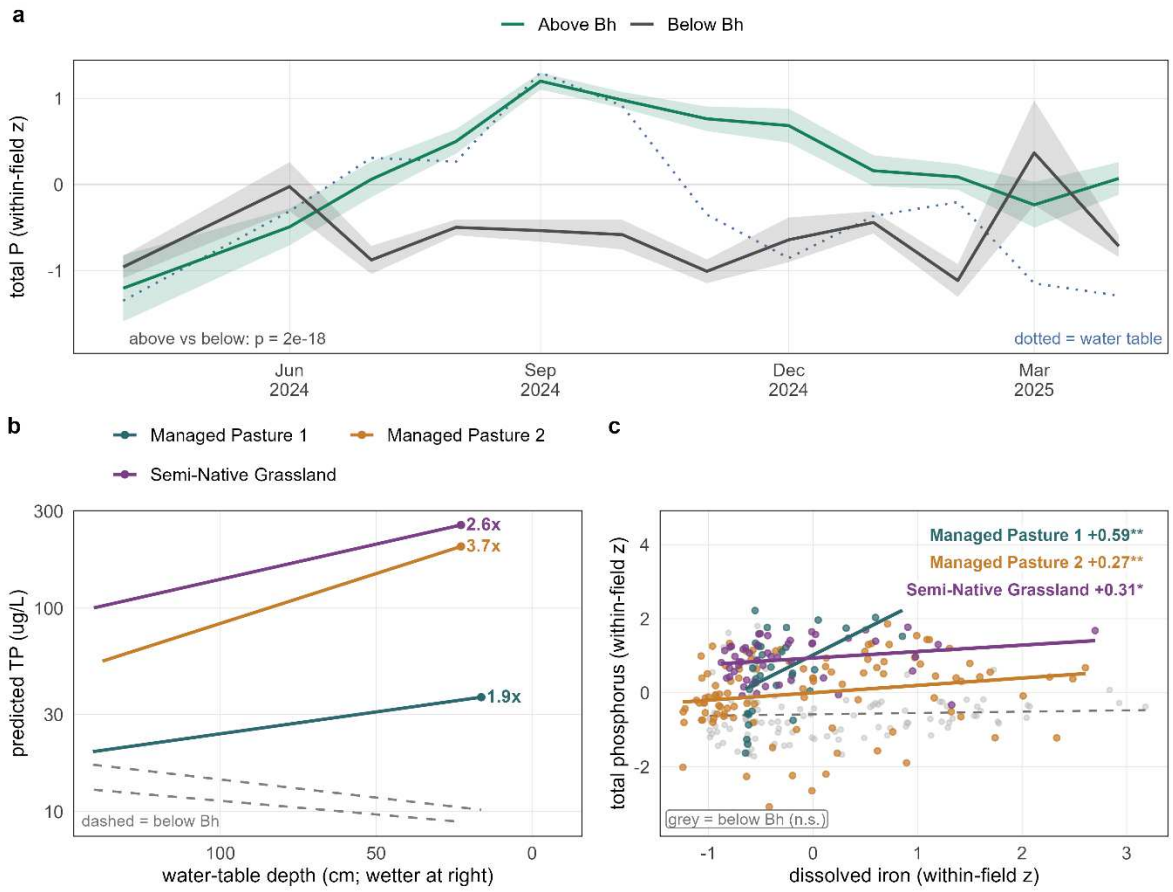
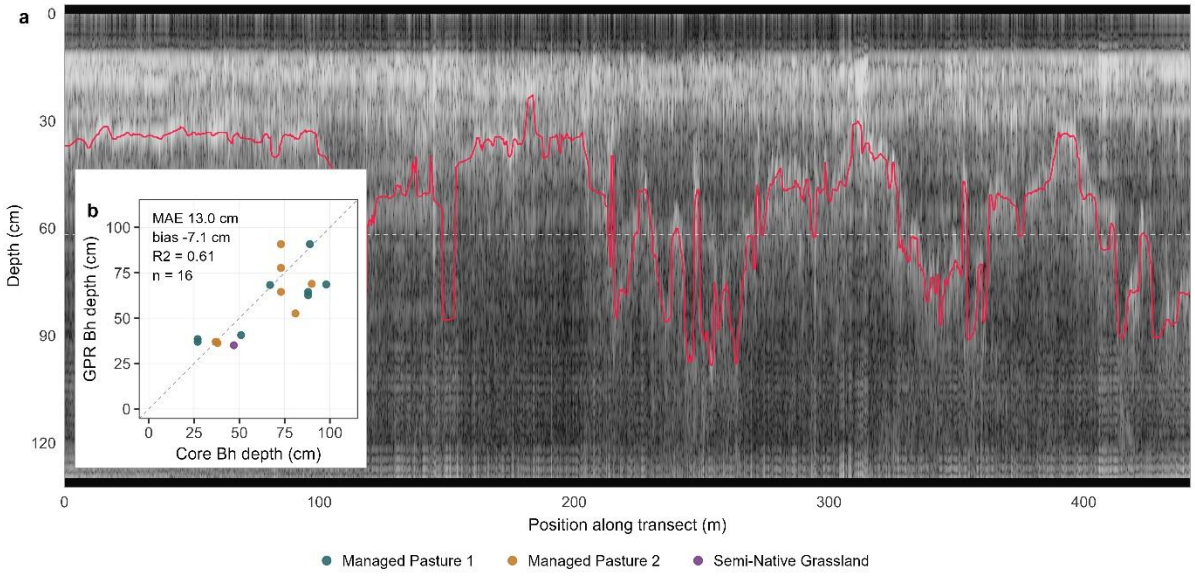


Figure 1. The buried spodic zone is the dominant P reservoir. (A) Depth-resolved Mehlich-3 P at each site — individual samples at their measured depth, with horizon-mean diamonds and 95% bootstrap confidence intervals; the shaded band marks the spodic (Bh + Bw) zone. The spodic zone (Bh and Bw, purples) carries the bulk of profile P. (B) Areal P reserve by horizon; the spodic zone (Bh + Bw) holds 60 to 78 percent of the profile total — a conservative floor, as the Bw was truncated at the 1 m core base (Methods).



533

534 *Figure 2. Pore-water P is gated by the water table and coupled to iron.* All sites pooled and
535 standardized within field. (A) Monthly above-Bh versus below-Bh total P with the water table
536 overlaid; above-Bh P lifts through the wet season while below-Bh stays flat (Mann-Whitney p =
537 2×10^{-18}). (B) Mixed-model-predicted total P against water-table position, by site, with the wet-
538 versus-dry fold-change (Managed Pasture 2 3.7×, Semi-Native Grassland 2.6×, Managed Pasture
539 1 1.9×); below-Bh predictions (dashed) are flat or declining. (C) Dissolved total P versus
540 dissolved iron, above and below the Bh; the two co-vary above the horizon at every site
541 (Spearman ρ = +0.27 at Managed Pasture 2, +0.59 at Managed Pasture 1, +0.31 at Semi-Native
542 Grassland; all $p < 0.05$) but not below.



543

544 *Figure 3. The reactive horizon is laterally continuous across the landscape.* Ground-penetrating
545 radar at 750 MHz along the best-covered transect (Managed Pasture 1, 442 m, 92.8 percent
546 bridged coverage): the Viterbi-tracked spodic reflector (red) and the core-mean Bh depth (dashed
547 white). Inset: radar-picked versus core-measured Bh depth at sixteen paired points across all
548 three sites (mean absolute error 13 cm, $R^2 = 0.61$). Two Managed Pasture 2 and Semi-Native
549 Grassland transects are in Extended Data Fig. 5.

550

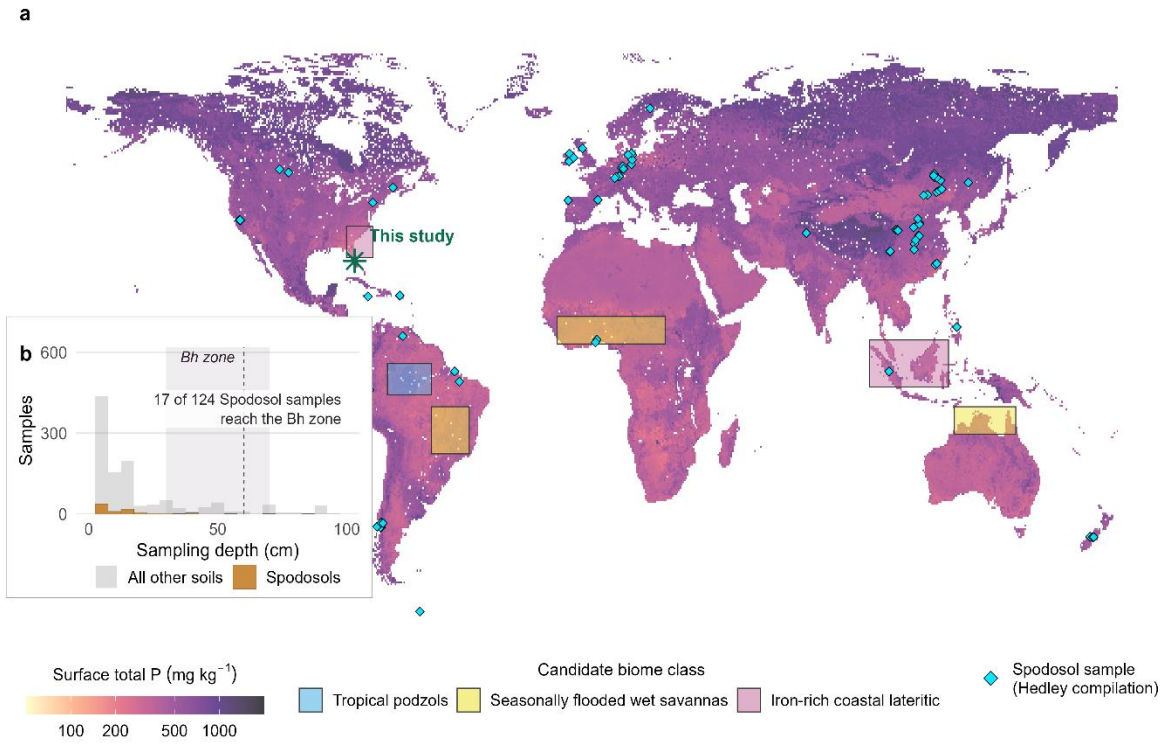
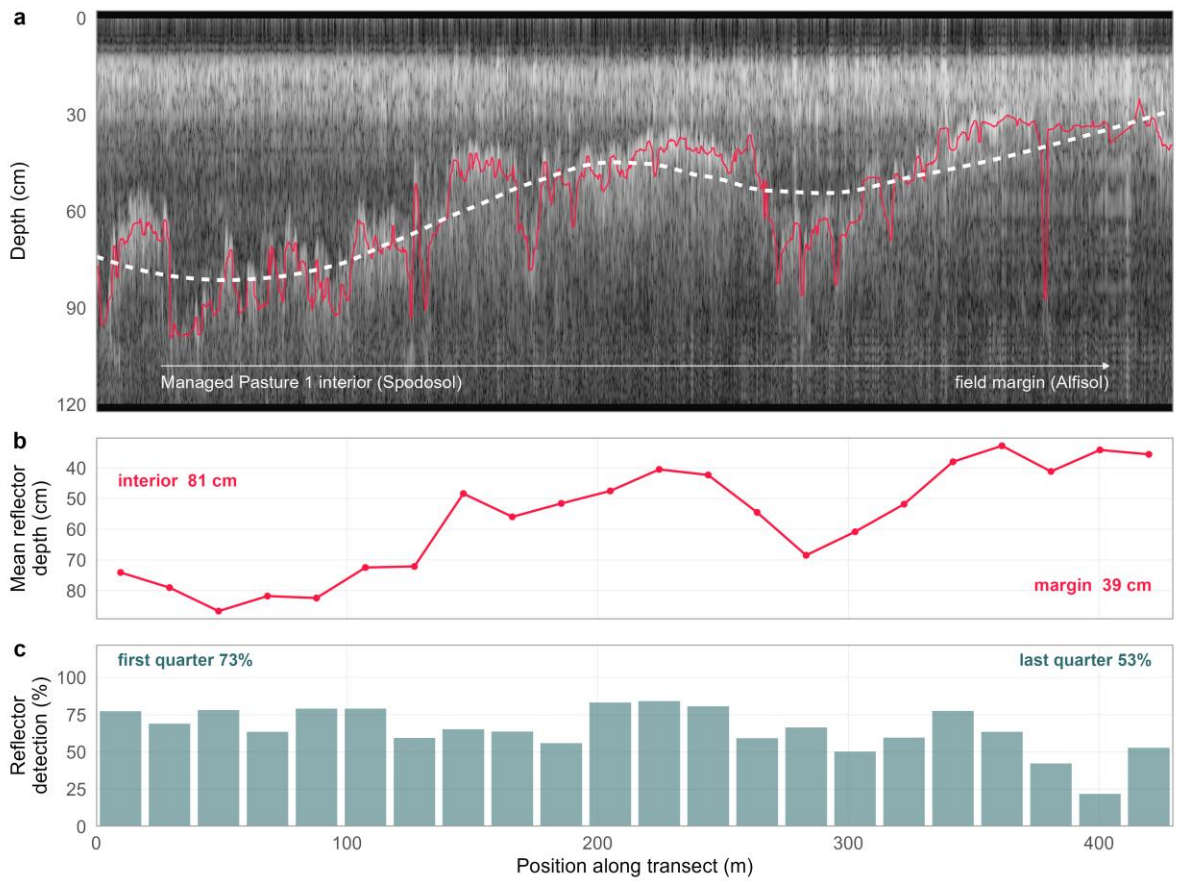
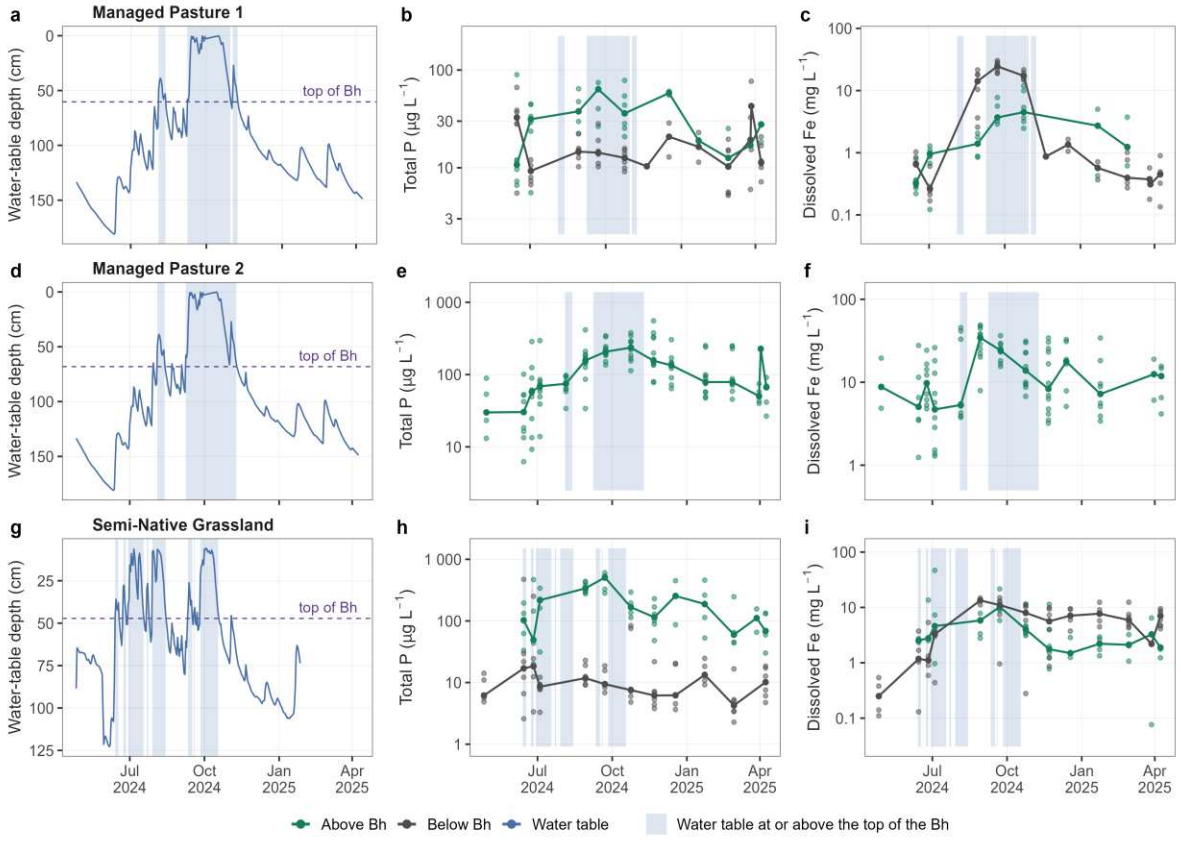


Figure 4. The reservoir's depth is largely unsampled in the global record. Map: global surface total P, with the locations of Spodosol samples in the global Hedley compilation and candidate biome classes where an iron-rich subsoil sits within a seasonal water table. The background field is a model prediction rather than an interpolation between the plotted points: it is the sum of six Hedley phosphorus fractions predicted at 0.5 degree resolution by the random-forest model of He et al. (2023), trained on the global Hedley compilation using climate, terrain and soil covariates (mean annual temperature and precipitation, elevation, clay and sand content, pH, soil organic carbon, soil order, bedrock, biome and net primary productivity); cells with no prediction are left white. Inset: sampling-depth distribution for Spodosols versus all other soils — only a small fraction of Spodosol samples reach the shaded Bh zone (median sampling depth about 10 cm), so the pool documented here is, at the global scale, largely unsampled.

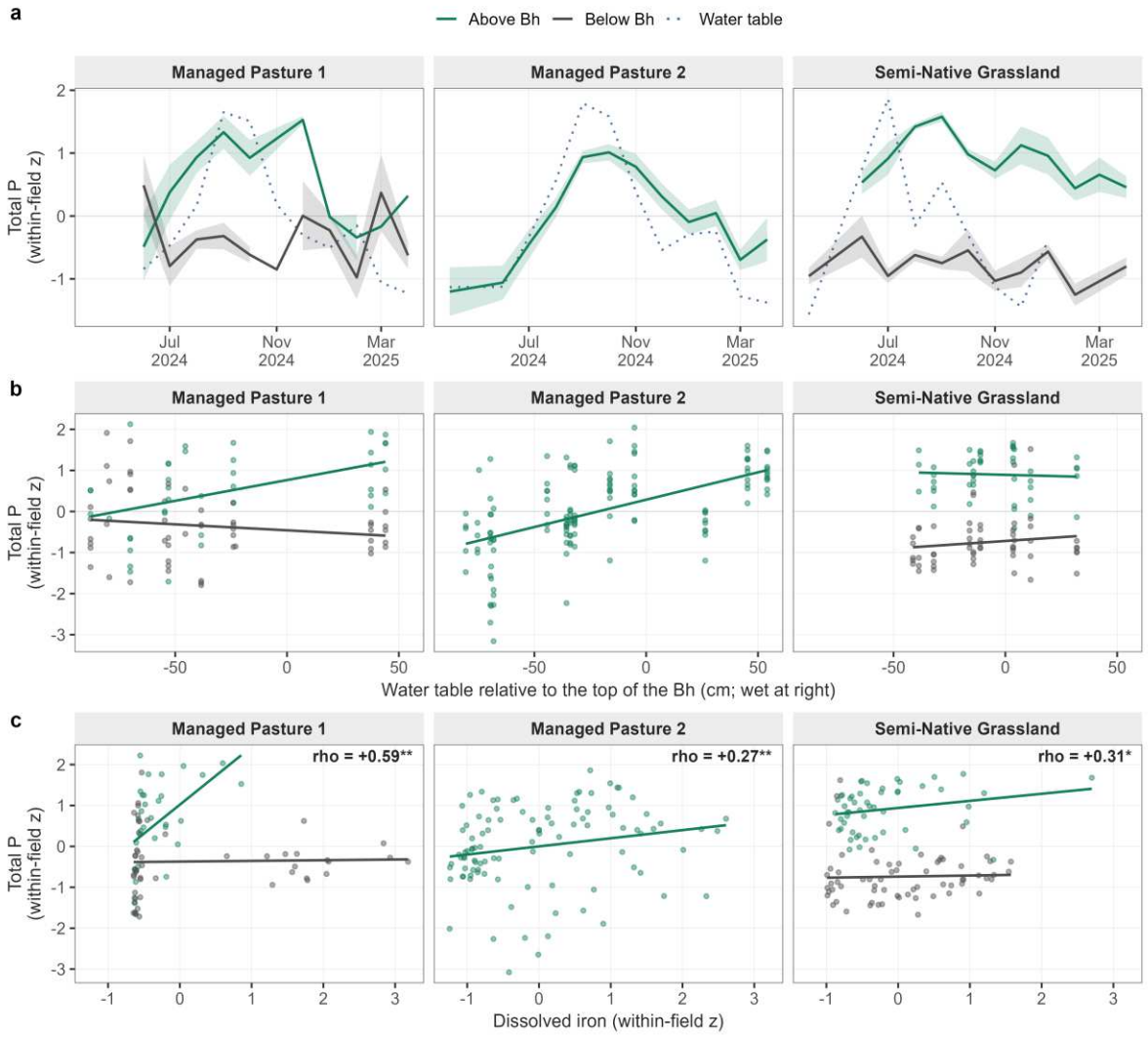
Extended Data



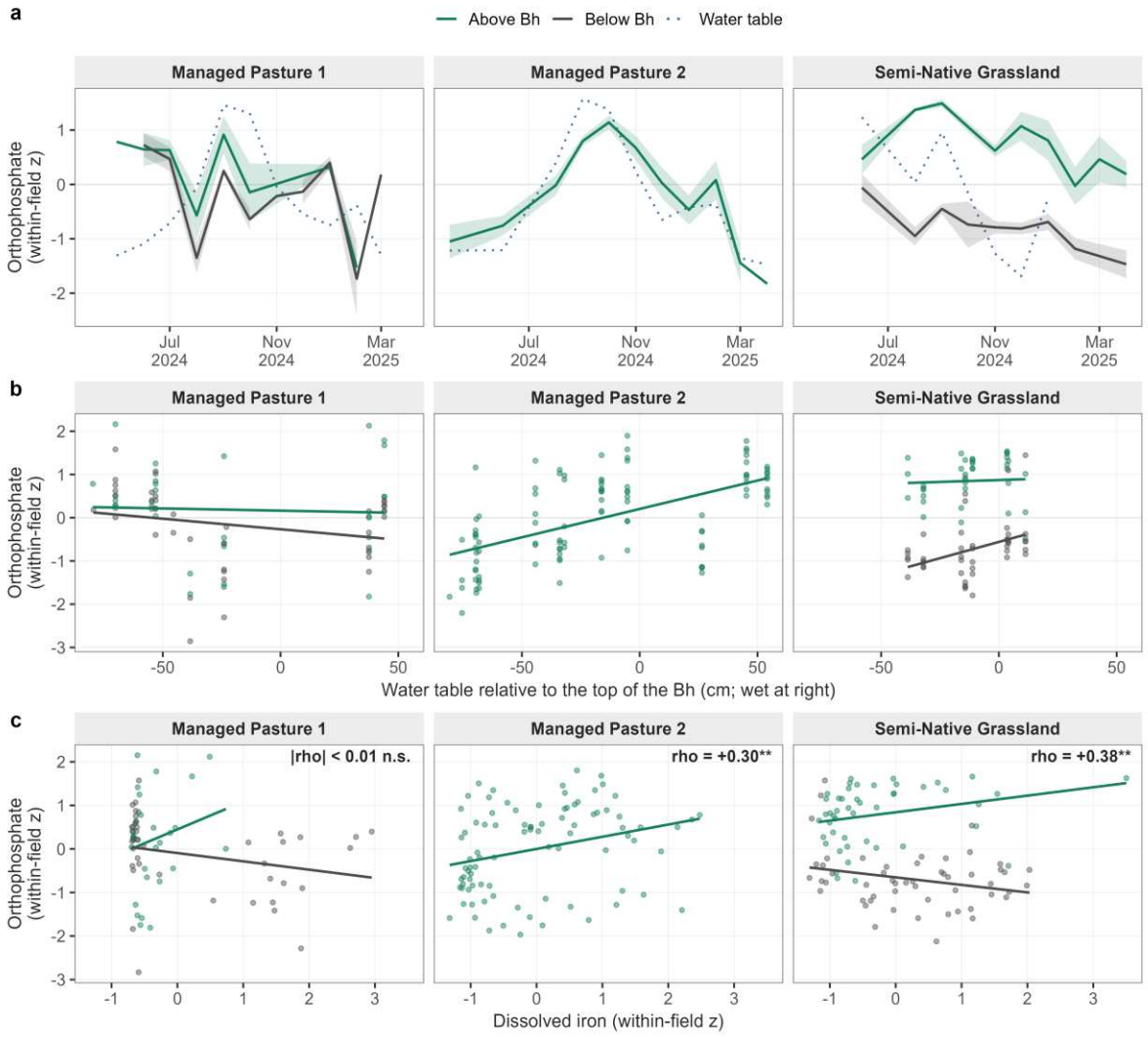
Extended Data Fig. 1 | Podzolization in reverse: the spodic rises and fades at the Alfisol boundary. Managed Pasture 1 transect p_r_0004, which runs from the pasture interior out to the field margin where the Spodosol grades into a neighbouring Alfisol. (A) Radargram with the Viterbi-tracked spodic reflector (red) and its loess trend (dashed white). (B) Mean reflector depth per 20 m bin: the spodic climbs from about 81 cm in the first quarter of the line to about 39 cm in the last. (C) Fraction of traces yielding a confident spodic pick, which falls from about 73 percent to about 53 percent over the same distance. The horizon does not simply get shallower; it thins and loses coherence as the soil ceases to be a podzol. Processing, velocity and tracker settings are identical to Fig. 3.



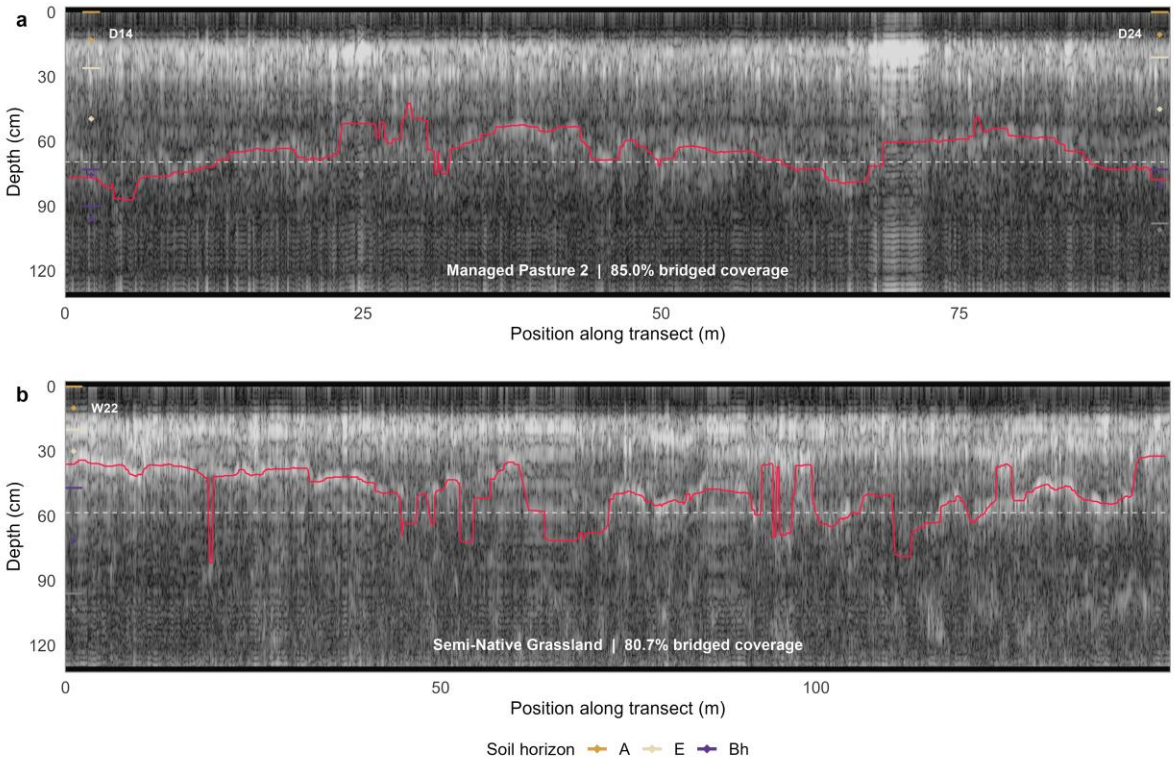
Extended Data Fig. 2 | The raw pore-water record behind the modelled response. Every lysimeter sample of total phosphorus and dissolved iron, by site, together with the daily water-table record that drives them. Rows are sites; reading across a row gives the driver and the response. Points are individual samples colored by position relative to the Bh (green above, grey below); heavy lines are per-date medians. Blue shading marks days on which the water table stood at or above the top of the Bh. Concentration axes are log-scaled. Nothing here is standardized or modelled: these are the observations from which the mixed-effects model of Fig. 2b is estimated. At Managed Pasture 2 both lysimeter depths sit above the spodic by design, so that site has no below-Bh series (Methods).



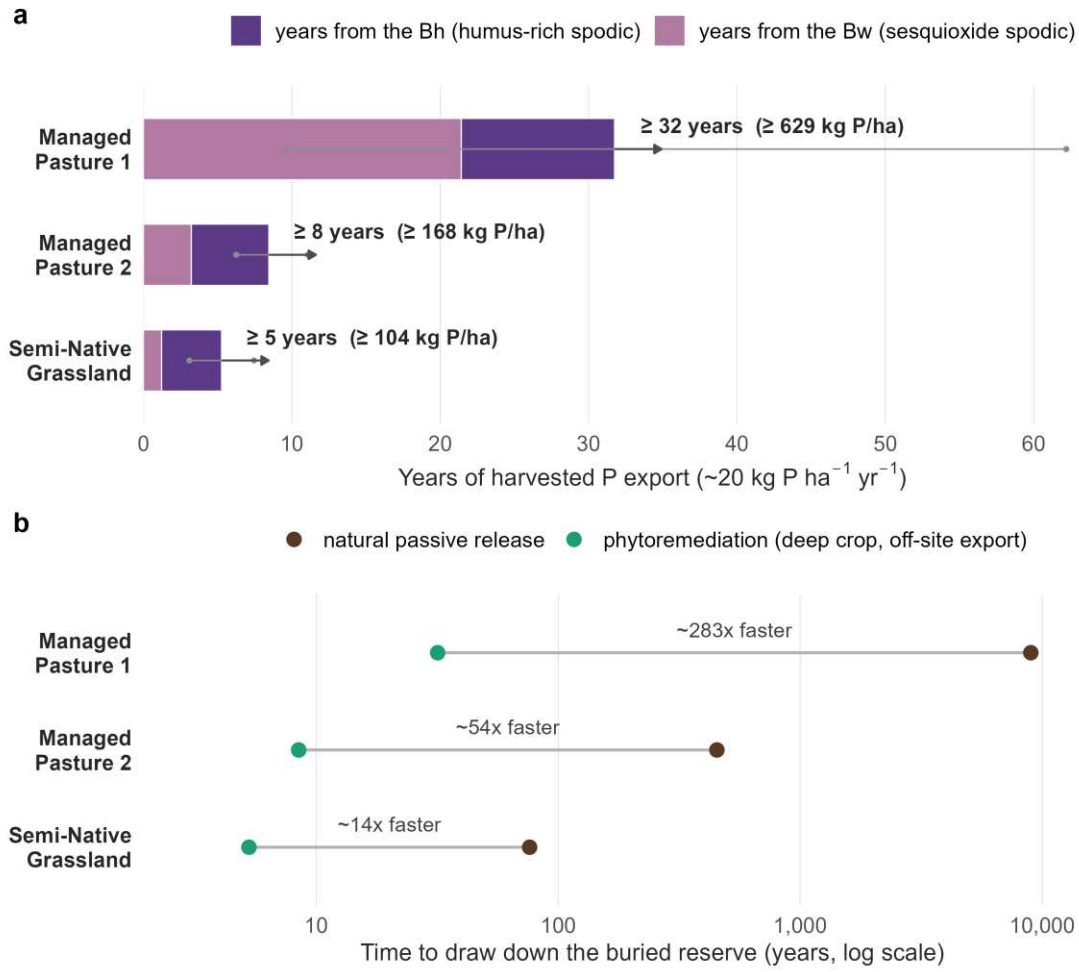
Extended Data Fig. 3 | Per-site pore-water total P (the by-site decomposition behind main Fig. 2). (A) Within-site-normalized above- versus below-Bh monthly time series with the water table. (B) Within-field standardized total P against water-table position relative to the Bh top, by site. (C) Dissolved Fe versus total P, above and below the Bh.



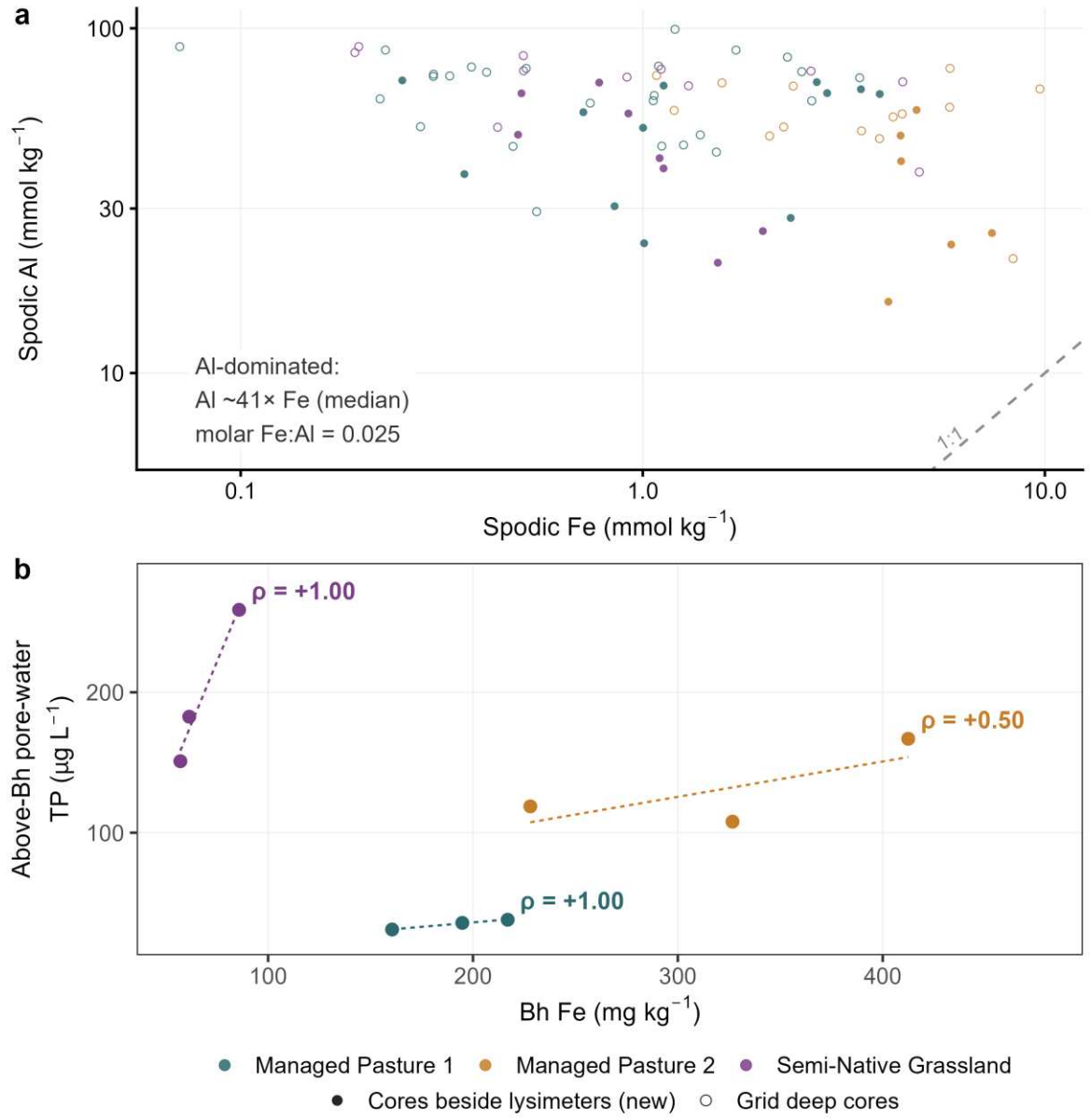
Extended Data Fig. 4 | Per-site pore-water orthophosphate. As Extended Data Fig. 3, for orthophosphate — the immediately plant-available form and the species released by reductive dissolution of Fe oxides. The contact pulse and Fe–orthophosphate coupling is clearest at Managed Pasture 2 and Semi-Native Grassland; Managed Pasture 1 orthophosphate is comparatively unresponsive, and the total-P signal carries that site.



Extended Data Fig. 5 | Ground-penetrating radar transects at Managed Pasture 2 and Semi-Native Grassland. As in main Figure 3 (the Managed Pasture 1 transect): 750 MHz radargrams with the Viterbi-tracked spodic reflector (red), the core-mean Bh depth (dashed white), and georeferenced cores overlaid. Bridged reflector coverage is 85.0% at Managed Pasture 2 and 80.7% at Semi-Native Grassland.



Extended Data Fig. 6 | The buried reserve as a management resource. a, The standing Bh + Bw reserve read as years of the companion crop's harvested P export (~20 kg P ha^{-1} yr^{-1}; Petticord et al. 2026b), split into the years supplied by the Bh and by the Bw. Grey ranges are bootstrap 95% confidence intervals. Arrows mark lower bounds: the Bw base was not reached within the 1 m cores, most so at Managed Pasture 2. b, Time to draw the same reserve down under passive natural release versus off-site export by a deep-rooted, flood-adapted crop, per site, on a log time axis. Both panels use the corrected spodic (Bh + Bw) reserves and the gross harvested export.



Extended Data Fig. 7 | Aluminum dominates the static spodic pool, but the water-table-gated release tracks iron. (a) Molar Fe versus aluminum in all spodic samples (Bh, Bw, and at Managed Pasture 1 the deeper Bt; n = 77), pooling the depth-resolved grid cores with a set of cores taken beside the lysimeter clusters. Nearly every sample lies far above the 1:1 line — aluminum is a median ~41× Fe (molar Fe:Al = 0.025) — consistent with the aluminum-

623 dominated Florida spodic Bh of Villapando and Graetz (2001). Neither Fe nor aluminum
624 abundance predicts total solid-phase P (pooled partial Spearman $|\rho| < 0.1$, not significant), as
625 expected of a pool set by illuvial loading history rather than current metal stoichiometry. (b)
626 Within each field, the co-located core whose Bh is richest in Fe underlies the lysimeter cluster
627 with the highest mean above-Bh pore-water total P (within-field Spearman $\rho = +1.0$ at Managed
628 Pasture 1 and Semi-Native Grassland, +0.5 at Managed Pasture 2; mean +0.83; field-centred
629 pooled $r = +0.50$ for total P and +0.44 for orthophosphate, $n = 9$ clusters across three fields).
630 Because aluminum (hydr)oxides are redox-insensitive while iron(III) reductively dissolves on
631 saturation, aluminum governs how much P the horizon can store whereas Fe governs how much
632 a rising water table can mobilize . Dashed lines are within-field linear fits (illustrative; $n = 3$
633 clusters per field, so the per-field coefficients are suggestive rather than individually significant).

634

635

636

Extended Data tables

Extended Data Table 1. Linear mixed-effects model, Type-III ANOVA. Model: log(total P) ~ water-table depth × lysimeter position × field, with crossed random intercepts for individual lysimeter and sampling date (n = 347; marginal $R^2 = 0.66$, conditional $R^2 = 0.78$).

Term	F	df (num, den)	p
water-table depth	7.50	1, 19.8	0.013
position	73.06	1, 130.7	< 0.001
field	40.70	2, 155.4	< 0.001
water-table depth × position	**15.70**	1, 291.9	**1×10^{-4}**
water-table depth × field	9.96	2, 177.7	1×10^{-4}
position × field	29.76	2, 130.1	< 0.001
water-table depth × position × field	**5.61**	2, 291.8	**0.0041**

The pre-specified water-table-by-position interaction is the primary inference; the pairwise Mann-Whitney, Wilcoxon and Spearman contrasts in the main text are reported uncorrected and read as corroborating.

Extended Data Table 2. Cross-correlation of above-Bh pore-water P with water-table position (monthly resolution.

Site	vs water table — total P	vs water table — orthophosphate
Managed Pasture 2	lag 0 months, r = 0.88	lag 0 months, r = 0.95
Managed Pasture 1	lag 0–1 months, r = 0.63	unresponsive (orthophosphate flat)
Semi-Native Grassland	lag ~2 months, r = 0.49	lag ~2 months, r = 0.49

The multi-month lag seen against an antecedent-precipitation index in an earlier analysis was the rain-to-water-table-rise delay; against the water table itself the release responds within the ~monthly sampling interval.

Extended Data Table 3. Spodic reserves and P-fraction sensitivity.

Site	Bh (kg/ha)	Bw (kg/ha)	Spodic Bh+Bw (kg/ha, 95% CI)	Bh/(A+Bh) median	Spodic/profile
Managed Pasture 1	205	424	629 (191–1232)	73%	78%
Managed Pasture 2	104	64	168 (124–219)	74%	74%
Semi-Native Grassland	80	24	104 (61–148)	83%	60%

Extended Data methods notes

- **Non-detects.** Orthophosphate and total-P non-detects were substituted at half the 4 µg L^{-1} reporting limit (2 µg L^{-1}).
- **Reserve computation.** Areal reserve = thickness-weighted mean Mehlich-3 P × assumed horizon bulk density (1.3 g cm^{-3} for A, 1.2 for E/Bh/Bw) × depth × 0.1, averaged over cores in which the horizon was measured; bootstrap 95% CIs from 2,000 resamples. Cores reached ~1 m and the Bw was the deepest horizon in every core that penetrated it (Managed Pasture 1 9/9, Managed Pasture 2 5/5, Semi-Native Grassland 3/3 of cores reaching the Bw), so Bw thicknesses — and thus Bw and spodic reserves — are truncated lower bounds, most so at Managed Pasture 2 (mean captured Bw ~22 cm, versus ~42 cm at Managed Pasture 1). Reported reserves are therefore conservative. Imputing each profile that did not reach the Bw its field-mean recovered Bw — a recovery-adjusted lower bound — raises the spodic reserves to 770, 206, and 120 kg P ha^{-1} at Managed Pasture 1, Managed Pasture 2, and Semi-Native Grassland, leaving the ranking unchanged.
- **Cores beside the lysimeters.** In addition to the depth-resolved grid cores, we collected one soil core beside each lysimeter cluster — three clusters per field (left, top, and right of the installation), plus an extra central core at Managed Pasture 1 — and analyzed each horizon for Mehlich-3 P, iron, aluminum, and pH. These targeted cores lack measured horizon thicknesses and so are used for concentrations and molar ratios only, not for areal reserves. Lysimeters were installed in clusters of four (numbered 1–4, 5–8, and 9–12), and each cluster was matched to its adjacent core; the aluminum-versus-Fe and core-iron-versus-release analyses (Extended Data Fig. 7) use this matching.

Extended Data references

Petticord, D.F., Boughton, E.H., Gough, A., Qiu, J., Reyes, A.L., Saha, A. et al. (2026b). P mitigation through hay harvest: addressing legacy P in subtropical pasture. Agriculture, Ecosystems & Environment 399, 110136. https://doi.org/10.1016/j.agee.2025.110136

Villapando, R.R., Graetz, D.A. (2001). P sorption and desorption properties of the spodic horizon from selected Florida Spodosols. Soil Science Society of America Journal 65(2), 331–339. https://doi.org/10.2136/sssaj2001.652331x

Supplementary Files

This is a list of supplementary files associated with this preprint. Click to download.

- nrreportingsummary.pdf